ARTICLE
Journal of Cellular Biochemistry 114:2363–2374 (2013)

Journal of Cellular Biochemistry

Heat and Radiofrequency Plasma Glow Discharge Pretreatment of a Titanium Alloy Promote Bone Formation and Osseointegration

Daniel E. MacDonald,[1,2,3]* Bruce E. Rapuano,[1] Parth Vyas,[1] Joseph M. Lane,[1] Kathleen Meyers,[1] and Timothy Wright[1]

[1]*Hospital for Special Surgery Affiliated With the Weill Medical College of Cornell University, 535 East 70th Street, New York, New York, 10021*

[2]*General Medical Research, James J. Peters VA Medical Center, 130 West Kingsbridge Road, Bronx, New York, 10468*

[3]*Langmuir Center for Colloids and Interfaces, Columbia University, 911 S.W. Mudd Building, Mail Code 4711, 500 West 120th Street, New York, New York, 10027*

ABSTRACT

Orthopedic and dental implants manifest increased failure rates when inserted into low density bone. We determined whether chemical pretreatments of a titanium alloy implant material stimulated new bone formation to increase osseointegration in vivo in trabecular bone using a rat model. Titanium alloy rods were untreated or pretreated with heat (600°C) or radiofrequency plasma glow discharge (RFGD). The rods were then coated with the extracellular matrix protein fibronectin (1 nM) or left uncoated and surgically implanted into the rat femoral medullary cavity. Animals were euthanized 3 or 6 weeks later, and femurs were removed for analysis. The number of trabeculae in contact with the implant surface, surface contact between trabeculae and the implant, and the length and area of bone attached to the implant were measured by histomorphometry. Implant shear strength was measured by a pull-out test. Both pretreatments and fibronectin enhanced the number of trabeculae bonding with the implant and trabeculae-to-implant surface contact, with greater effects of fibronectin observed with pretreated compared to untreated implants. RFGD pretreatment modestly increased implant shear strength, which was highly correlated ($r^2 = 0.87–0.99$) with measures of trabecular bonding for untreated and RFGD-pretreated implants. In contrast, heat pretreatment increased shear strength 3–5-fold for both uncoated and fibronectin-coated implants at 3 and 6 weeks, suggesting a more rapid increase in implant-femur bonding compared to the other groups. In summary, our findings suggest that the heat and RFGD pretreatments can promote the osseointegration of a titanium alloy implant material. J. Cell. Biochem. 114: 2363–2374, 2013.

KEY WORDS: DENTAL IMPLANT; FIBRONECTIN; OSTEOBLAST; CELL DIFFERENTIATION; BONE MINERALIZATION; OSSEOINTEGRATION

The success of orthopedic and dental implants depends on the intimate relationship between the implant surface and surrounding bone. Unfortunately, implant loosening is still a significant problem. In fact, 25% of hip replacement surgeries reviewed in 2003 were revisions due to previous implant failure [Webster, 2003]. Despite the long-term favorable outcome of most dental implant procedures [Adell et al., 1990], 10% of dental implants fail within 5 years [Hardt et al., 2002] with decreased survival rates for revision surgeries of 71–83.5% over a 3.5–6 year period [Grossmann and Levin, 2007; Machtei et al., 2008]. Second revisions fail at an even higher rate (60.0% at 1 year) [Machtei et al., 2011].

Although improvements have been made in implant design, they remain biocompatible but not biomimetic. The quality and quantity of bone formation at the implant-skeletal interface are important to insure long-term success [Johansson and Strid, 1994]. Strategies that promote the recruitment, attachment, and function of local osteoblasts at the interface are likely to lead to early implant stability and enhanced bone repair, thus reducing patient recuperation time.

The authors declare that they have no conflict of interest.

Grant sponsor: NIH; Grant number: RO1 DE017695; Grant sponsor: National Center for Research Resources, NIH; Grant number: C06-RR12538-01.

*Correspondence to: Dr. Daniel E. MacDonald, Hospital for Special Surgery, 535 East 70th Street, New York, NY 10021. E-mail: dem14@columbia.edu

Manuscript Received: 22 April 2013; Manuscript Accepted: 29 April 2013

Accepted manuscript online in Wiley Online Library (wileyonlinelibrary.com): 3 May 2013

DOI 10.1002/jcb.24585 • © 2013 Wiley Periodicals, Inc.

Commercially pure titanium (cpTi) and titanium alloys are widely employed as implant materials [Larsson et al., 1996]. Ti6Al4V alloy is used in orthopaedic [Lausmaa, 2001] and dental implants [Morris et al., 2001]. Both titanium and its alloys form an active oxide layer that interact with extracellular matrix proteins produced by cells and cell surface proteins, thereby providing an interface biocompatible with peri-implant tissues [Kasemo, 1983; Imam and Fraker, 1996]. The surface oxide of Ti6Al4V is similar to that of cpTi except that it is enriched with aluminum-oxide when present in air [MacDonald et al., 2004]. The alteration of this surface can have pronounced effects on protein adsorption, cell-substrate interactions, and tissue development [Sousa et al., 2008]. However, the relationship between the alloy's surface oxide properties and its osseointegration has not been elucidated. By exploiting the dynamic nature of the oxide surface layer, it may be possible to develop an implant that actively interacts with the surrounding bone cells to stimulate their maturation and production of a new mineralized matrix.

Many strategies have been employed to modify the implant surface to enhance osseointegration, including deposition of peptide monolayers, surface roughening, ion beam deposition, chemical methods (acid–base etching, electrochemistry), nanopartical attachment, inorganic crystalline deposition, and textured nanosurfaces [Mendonca et al., 2008; Dohan et al., 2010]. Although plasma spraying of calcium phosphate (hydroxyapatite) coatings onto the titanium surface has been reported to enhance osteoconductivity [Dhert et al., 1998], human studies have shown coating dissolution from soluble nonapatitic phases shortly after implantation [MacDonald et al., 2000, 2001]. Bioactive adhesive proteins, such as the extracellular matrix protein fibronectin, have been used to facilitate the surface attachment of osteogenic cells [MacDonald et al., 1998, 2002; Rapuano et al., 2004; Harbers and Healy, 2005]. Fibronectin is thought to play an essential role for skeletal development in regulating osteoblast differentiation and mineralization [Moursi et al., 1996]. Fibronectin binds rapidly and irreversibly to TiO_2 [MacDonald et al., 2002] so that the protein can be efficiently adsorbed to titanium materials without the use of intervening chemical coupling agents.

We believe that a compound surface strategy is necessary to improve implant fixation. The initial strategy is to create an oxide structure and chemistry that will encourage protein binding in an open orientation that reveal peptide binding sites accessible to osteoblast integrin binding receptors, thus promoting improved receptor-binding activity. The second strategy is to employ an extracellular matrix protein with demonstrated stimulatory effects on osteoblast attachment and maturation. Such an approach would create a truly bioactive surface.

We previously examined the effects of modifying Ti6Al4V surface oxide properties, followed by coating the material with fibronectin, on the protein's bioactivity toward osteoblasts [MacDonald et al., 2004, 2011; Rapuano and MacDonald, 2011; Rapuano et al., 2012a]. Pretreating the surface oxide with heat or radiofrequency plasma glow discharge (RFGD) increased the oxide's negative net charge [MacDonald et al., 2011], markedly increased the number of osteoblasts that attached to surface adsorbed fibronectin [Rapuano and MacDonald, 2011], and increased the exposure of fibronectin's integrin binding domain to enhance its binding to $\alpha_5\beta_1$ integrins [Rapuano et al., 2012a]. Later studies showed that fibronectin coating, heat and RFGD pretreatments each increased the expression of osteoblast gene markers, suggesting a stimulation of osteoblast differentiation [Rapuano et al., 2012b,c]. Pretreatments also increased osteoblast gene expression for fibronectin-coated disks more than uncoated disks, suggesting a pretreatment-induced specific enhancement of fibronectin's bioactivity [Rapuano et al., 2012c] putatively via conformational changes induced by the modified oxide [Rapuano et al., 2012a].

In a more recent study, we showed that these same pretreatments of Ti6Al4V stimulated bone mineral formation in cultures of attached MC3T3 osteoprogenitor cells in vitro [Rapuano et al., 2013]. To determine if the pretreatments of the alloy also affected its osseointegration in vivo, a rat model was used to measure new bone formation and implant-bone bonding strength. Titanium alloy rods were pretreated, coated with fibronectin or left uncoated, placed in the rat femoral medullary cavity, and analyzed after 3 and 6 weeks. New bone formation around the implant was measured using histomorphometry and implant bonding strength was measured using a pull-out test. Demonstrating that the pretreatments of the alloy increased these quantitative and qualitative measures of osteogenesis on the implant surface in vivo was used to test the hypothesis that the treatments can enhance the osseointegration of the implant material.

MATERIALS AND METHODS

MATERIALS

Skeletally mature male Sprague–Dawley rats were purchased from Harlan Labs (South Easton, MA). 1.5 mm cortical bone drills were acquired from Glidewell Labs (Newport Beach, CA). Human plasma fibronectin was obtained from Sigma–Aldrich (St. Louis, MO). Methyl methacrylate solution was purchased from Polysciences, Inc. (Warrington, PA). Butylmethacrylate, dibenzoyl peroxide, and polyethylene glycol solutions were all from Sigma–Aldrich. Solutions of ethanol, isopropanol, and xylene were from Pharmco-AAPER (Brookfield, CT). Ti6Al4V wire was purchased from Industrial Tool & Die Co. (Troy, NY).

PREPARATION OF IMPLANTS

To prepare cylindrical Ti6Al4V implant rods, lengths of circular wire (1 m long by 1.5 mm diam.) were manually polished to insure an even surface finish. The samples were then cut into 15 mm rods. A small "location notch" was placed in each rod from 1 to 2.5 mm from one end to delineate where it would be held in the ceramic sample holder during subsequent heat and RFGD surface pretreatments (see below). For consistency, untreated samples were also notched.

The rods were then passivated to form a stable surface oxide layer, dried and transferred into acid-washed scintillation vials in a HEPA filtered isolation hood, dry heat sterilized, and stored closed in an auto-desiccator cabinet as previously described [MacDonald et al., 2004, 2011]. The rods were then pretreated with heat or RFGD or left untreated [MacDonald et al., 2011]. To insure equal circumferential treatment, ultra-high temperature glass-mica ceramic (Corning Glass, Corning, NY) holders were fabricated to keep the

rods vertically supported. The rods were heated to 600°C in air for 1 h in a tube furnace and slowly cooled to room temperature [MacDonald et al., 2004]. RFGD pretreatments were performed using a modified Harrick RF unit (Ossining, NY; PDC 002) with a quartz chamber. Implants were inserted into the RF unit. Once a vacuum of 1,600 mTorr was obtained, pre-filtered oxygen was bled into the system at ~250 ml/min, and the rods were treated with a 13.56 mHz RF power-generated oxygen plasma for 5 min at 29.6 W [MacDonald et al., 2011]. Passivated rods (untreated) were used as a control group. All samples were sterilized under dry heat as previously described [MacDonald et al., 2004, 2011]. After treatment, the sterile rods were incubated in 20 ml glass vials, submerged (using sterile technique) in sterile 1X PBS (or the same solution containing 1 nM fibronectin) and incubated overnight on a platform shaker under a cell culture hood at room temperature. There were six experimental groups: untreated without a fibronectin coating (no fibronectin), untreated with a fibronectin coating (fibronectin), heat (no fibronectin), heat (fibronectin), RFGD (no fibronectin), and RFGD (fibronectin). A sample size of 5–8 animals was used for each group.

SURFACE ANALYSIS—ATOMIC FORCE MICROSCOPY IMAGING FOR ROUGHNESS ANALYSIS

Atomic force microscopy (AFM) was used to image untreated control and pretreated alloy rods to determine their surface topography. An NTEGRA Prima Scanning Probe Laboratory (NTMDT, Zelenograd, Russia) AFM system was employed in tapping mode under ambient conditions. Several random 10 μm $\times$ 10 μm and 1 μm $\times$ 1 μm areas on two alloy rods were scanned for each of the untreated and pretreated groups and a root mean square (RMS) and average (Ra) roughness analysis was performed, as we have previously described [MacDonald et al., 2004, 2011].

SURGICAL PROCEDURE

One hundred skeletally mature (250–275 g) Sprague–Dawley rats were used. All experiments were approved by the Institutional Animal Care and Use Committee of the Hospital for Special Surgery (IACUC protocol #04-11-05R). Surgery was performed under general anesthesia administered via intra-peritoneal injection with a combination of Ketamine (Ketaset, 100 mg/ml at 75 mg/kg, Fort Dodge Animal Health, Fort Dodge, IA) and Xylazine (Rompun 20 mg/ml at 7 mg/kg, Shenandoah, IA) Additional anesthesia was provided by administration of isoflurane via nose cone. The surgical site and wide margins were clipped free of hair, scrubbed three times with Dermachlor (Chlorhexidine medical scrub 2%), and disinfected with 70% alcohol. The legs were shaved for bilateral operations. A 3–4 mm medial incision was made to expose the head of the ligamentum patellae and displace it laterally to expose the distal femur. A pilot hole was made through the cortical bone in the intercondylar notch with a 22 gauge needle. The medullary canal was negotiated with a blunted 23 gauge IV needle and widened with successive blunted 20 gauge and 18 gauge IV needles creating a channel into the canal. The channel was reamed to a depth of 15 mm with an MD10 implant surgical system (Nouvag AG, Goldach, Switzerland) and bone drill (1.5 mm diam.) and cooled with sterile saline. The rod was submerged 1 mm below the intercondylar cartilage surface using a small "location notch." Radiographs were performed to insure proper placement. The patella ligament and skin incisions were separately sutured (Vicryl 4/0, Ethicon) and the rats were given an analgesic post-surgery. This non-weight-bearing intrafemoral implant model allows direct investigation of implant surface-bone interaction in the absence of compounding biomechanical factors [Barber et al., 2007].

Rats were placed post-surgically in a warmed ICU cage and provided SQ fluid support with sterile lactate Ringer's 20 ml bolus administered subcutaneously preoperatively. An initial dose of Buprenophine (Buprenex, Reckitt Benckiser Healthcare Ltd, Hull, England) 0.05 mg/kg SC was administered postoperatively upon anesthetic recovery and then at 0.05 mg/kg SC every 8–12 h for 48 h. Animals were then housed in clean cages in an environmentally controlled room with steady temperature and humidity. After 3 or 6 weeks, they were euthanized in a CO_2 chamber, and femurs were harvested and cleaned of attached tissue. Right legs, used for histomorphometry, were placed in 95% ethanol and refrigerated. Left legs, used for biomechanical testing, were wrapped with normal saline soaked gauze and stored at −20°C.

QUANTITATION OF NEWLY FORMED BONE IN CONTACT WITH THE IMPLANT

Femora were treated with the methacrylate (MMA) method [Erben, 1997], using dehydration in increasing concentrations of ethanol, isopropanol, and then xylene, followed by infiltration with three MMA solutions for 3 days each. The femur was polymerized with a solid Epon solution in an embedding case. The sample was embedded and polymerization was activated by adding dimethyl-p-toluidine to cold MMA solution. The case was sealed tightly and placed in the freezer at −20°C for 3 days.

Polymerized blocks were cut from the cases and sectioned on a diamond saw (Buehler, Inc., Lake Bluff, IL). X-rays of the sample blocks helped locate the rod relative to the femur. Coronal cross-sections were taken at 25%, 50%, and 75% of the rod length measured from the distal end and imaged by environmental scanning electron microscopy (ESEM; FEI, Quanta 600, Peabody, MA) in the secondary electron mode. All specimens were imaged at 20× and a voltage of 20 kV [MacDonald et al., 2000]. The number of trabeculae bonding to the implant surface, the total length of trabeculae-to-implant surface contact (measured as the sum of the thicknesses of all of the trabecular struts at their points of contact with the implant) and the total circumferential length and area of newly formed bone attached to the implant ("implant bone") were quantified with Bioquant-2 Image analysis software (R&M Biometrics, Inc., Nashville, TN). The number of bonding trabeculae and the length of trabecular surface contact may vary as a function of the cross-sectional length or area of newly formed bone on the implant surface due to the release of paracrine osteogenic factors from bone cells on the implant surface. Therefore, both measures of trabecular-implant bonding were also normalized to the length or area of implant bone. Data were averaged for the three cross-sections and presented as mean $\pm$ SE.

FTIR MEASUREMENTS OF BONE HEALING

Histologic PMMA samples were cut into 3 mm cross-sections, polished, and the implants carefully pushed out employing a 1 mm diameter carbide rod mounted into a lathe. Two micrometer thick sections for FTIR imaging were obtained from PMMA-embedded

mineralized tissue specimens. Sections were mounted on barium fluoride windows and scanned using a Perkin Elmer (Waltham, MA) Spectrum-Spotlight-100 system at 4 cm^{-1} spectral resolution and 25 μm pixel size in the transmittance mode. Infrared images were analyzed using ISYS Chemical Imaging software (Spectral Dimensions [presently Malvern], Olney, MD). All images were visually evaluated by the distribution of the following FTIR parameters: mineral/matrix ratio and acid phosphate content [Boskey and Mendelsohn, 2005].

MEASUREMENTS OF BONE–IMPLANT SHEAR STRENGTH

The shear ("pull-out") force to detach the rod from its femoral site was measured. Three millimeters of the rod was exposed through the distal end of the femur by carefully removing bone circumferentially with a round bur mounted on a rotary tool. Each femur was then potted in epoxy. All samples were stored at −20°C until tested. For testing, the rod was pulled out of the femur using a servohydraulic load frame (MTS, Eden Prarie, MN). A custom self-aligning fixture was used to ensure pure uniaxial force. Load was applied using a displacement rate of 0.5 mm/min. Load and piston displacement were recorded, and peak failure load was determined.

STATISTICAL ANALYSIS

Data were normally distributed. Statistical comparisons among groups were performed using an ANOVA with the alpha level set at 0.05. Only the results of the post tests (Bonferroni) for multiple comparisons are presented.

RESULTS

RMS roughness analyses of the surfaces of untreated and pretreated rods were performed by AFM. We have previously shown using AFM that alloy disks exposed to RFGD pretreatment exhibited a relatively smooth surface topography that was identical to that of untreated specimens, whereas heat-pretreated surfaces displayed numerous oxide projections 50–100 nm in diameter [MacDonald et al., 2011]. AFM surface analysis of alloy rods also showed that RFGD pretreatment had little or no effect on surface topography. In contrast, the preheated implants were covered with a high density of rounded elevations not observed on the untreated or RFGD-pretreated surfaces, similar to what we have previously reported for preheated alloy disks [MacDonald et al., 2011]. RMS values ranged from 25 to 44 nm (R_a = 19–35 nm), 49–51 nm (R_a = 39–41 nm), and 70–88 nm (R_a = 54–70 nm) for untreated, RFGD-pretreated and heat-pretreated rods, respectively.

Electron microscopic images demonstrated that new bone had formed around part of the circumference of untreated and treated rods during the 6 week experiment (Fig. 1; red arrows). Little or no space was observed between the bone and the rod, and an anchoring network of trabecular "struts" was observed (Fig. 1; black arrows). A narrow zone of demarcation was often observed between the circumferential bone and the surface of the contacting trabeculae (Fig. 1; yellow arrows). This zone contained lower density bone compared to either the struts or the bone attached to the surface (Fig. 1; yellow arrows). Some trabecular struts had also joined to the outer band of femoral cortical bone (Fig. 1; green arrows).

The pretreatments increased the number of trabeculae observed to bond to the implant at 3 or 6 weeks by 25–100% compared to untreated specimens for both fibronectin-coated or uncoated specimens. Fibronectin produced a general pattern of increases in the number of trabeculae bonded at 6 weeks (Fig. 2A). Fibronectin had greater apparent effects on the number at 3 and 6 weeks for RFGD-pretreated compared to untreated implants. RFGD pretreatment had equivalent or greater effects on the number of trabeculae compared to the heat pretreatment. RFGD pretreatment caused a significant doubling of trabeculae in the presence (3 weeks) or absence (6 weeks) of fibronectin. No consistent differences were found between 3 and 6 week results (Fig. 2A).

The number of contacting trabeculae was also normalized to the length of bone that had formed around the implant's circumference (Fig. 2B). Neither treatment significantly increased the length of bone compared to untreated specimens (unpublished results). However, significant increases were observed in the number of bonded trabeculae/mm of implant bone (50–140%) for pretreated compared to untreated (fibronectin-coated or uncoated) implants at 3 and 6 weeks. Although a pattern of increases in the number of bonded trabeculae/mm of implant bone were observed for fibronectin-coated compared to uncoated specimens for almost every group among the two time intervals, fibronectin's apparent effects at 3 and 6 weeks were generally greater for pretreated compared to untreated implants. The magnitude of the heat pretreatment effect was equal to or greater than that of RFGD pretreatment (Fig. 2B). No consistent differences in the number of trabeculae/mm implant bone were found between the 3 and 6 week specimens.

The pretreatments increased the length of trabeculae-to-implant surface contact after 3 or 6 weeks by 25 to nearly 200% compared to untreated specimens with or without a fibronectin coating (Fig. 3A). Both pretreatments promoted greater % increases in trabecular surface contact (Fig. 3A) at 3 weeks than in the number of trabeculae bonding to the implant (Fig. 2A). Surface contact between trabeculae and the implant appeared to be greater in general for fibronectin-coated compared to uncoated specimens at 6 weeks (Fig. 3A). These effects of fibronectin on trabecular surface contact at 3 and 6 weeks were greater for RFGD-pretreated compared to untreated implants. The RFGD pretreatment appeared to exert generally greater effects on trabecular surface contact compared to the heat pretreatment. RFGD pretreatment of fibronectin-coated implants promoted significant increases in trabecular surface contact by two- and threefold over that of the untreated condition at 6 and 3 weeks, respectively (Fig. 3A). No significant differences were found between the 3 and 6 week trabeculae-to-implant surface contact under the same conditions.

When normalized to the length of bone that had formed around the implant's circumference, the pretreatments promoted significant increases of 65–200% in implant-trabeculae surface contact at 3 and 6 weeks for fibronectin-coated or uncoated specimens (Fig. 3B). Both pretreatments promoted greater % increases in trabecular contact/mm implant bone (Fig. 3B) at 3 weeks compared to the number of trabeculae bonding to the implant (Fig. 2B). A pattern of higher levels of implant-trabeculae surface contact/mm of implant bone were generally found for implants coated with fibronectin compared to uncoated implants. This pattern of effects of fibronectin on trabeculae surface contact/mm of implant bone at 3 and 6 weeks was generally

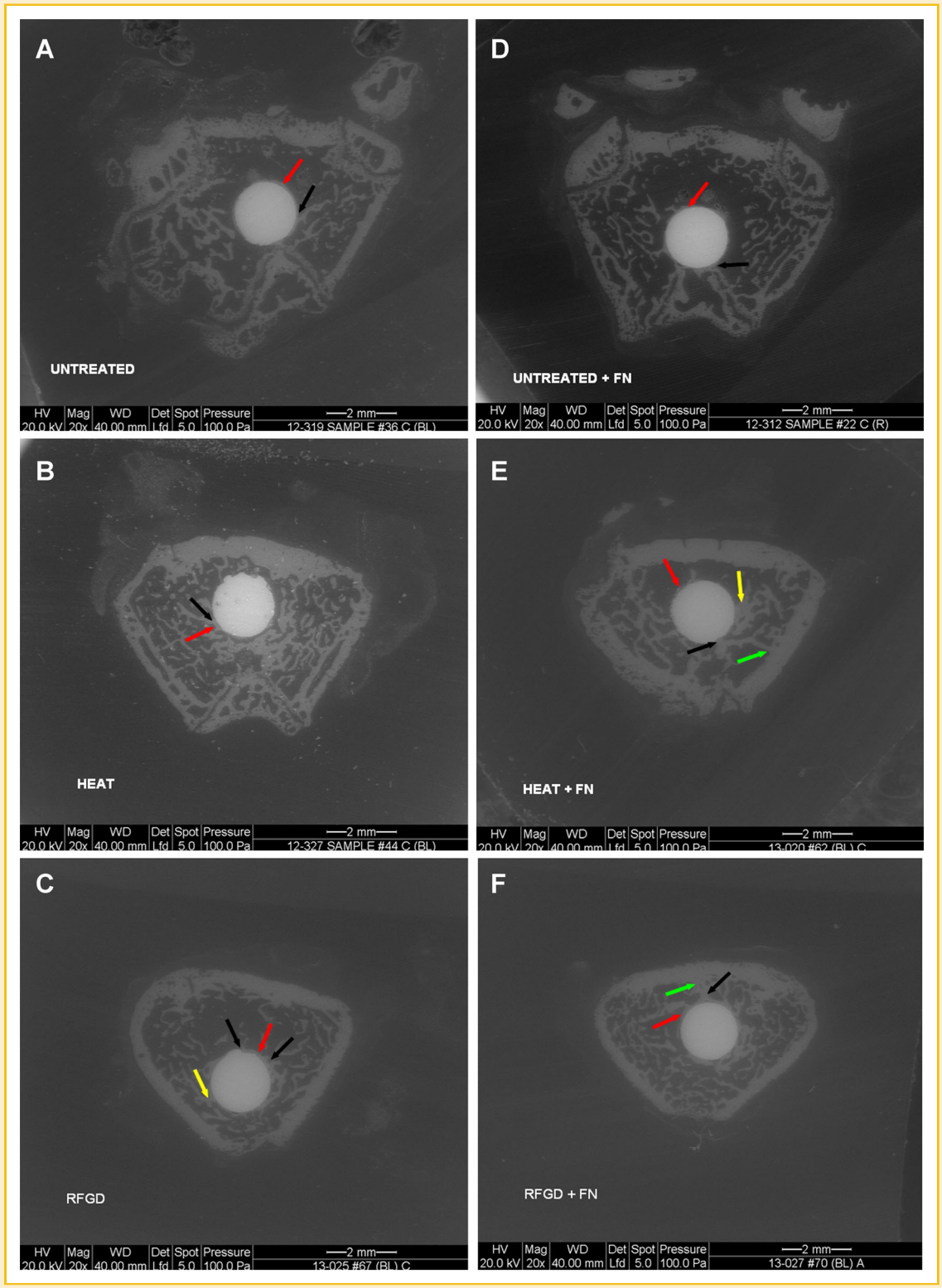

Fig. 1. Electron microscopic images of coronal sections 6 weeks following implantation. Implants were untreated (A,D) or pretreated with heat (B,E) or RFGD (C,F), left uncoated (A–C) or coated overnight with 1 nM fibronectin (D–F). Micrographs are shown for sections taken near the distal end of the femur. Red arrows show newly formed bone. Black arrows show areas in which newly formed bone has become anchored to trabeculae; green arrows show trabeculae that also appear to be joined to the outer band of cortical bone. Yellow arrows show a zone of demarcation between the bone surface around the implant's circumference and the surface of the trabeculae with which it appears to be in contact. FN, fibronectin; HEAT, heat pretreatment; RFGD, radiofrequency plasma glow discharge pretreatment.

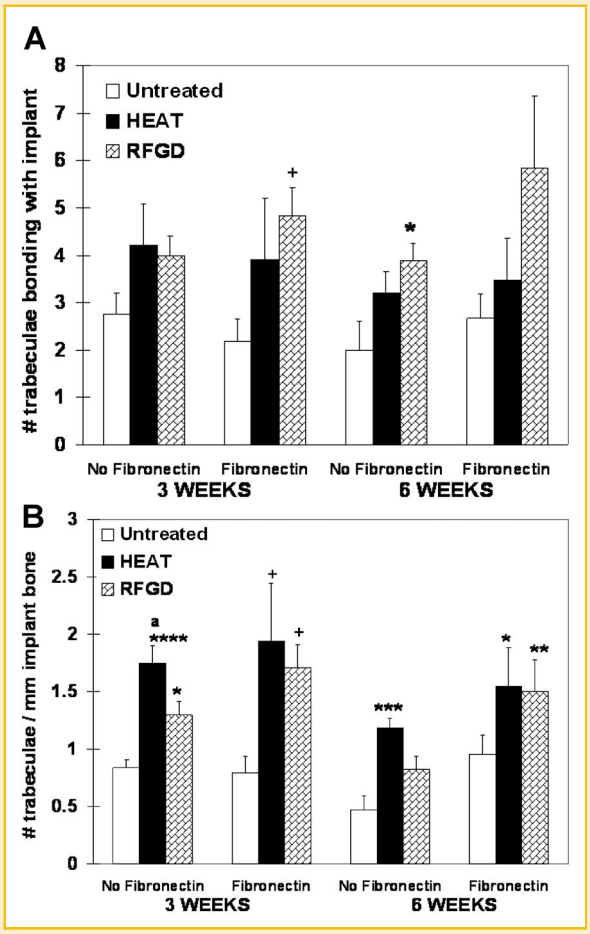

Fig. 2. Effects of heat and RFGD pretreatment on the number of trabeculae joined to the implant surface. A: Number of trabeculae bonded to the implant per cross-section. B: Number of trabeculae bonded to the implant/length (mm) of surface implant bone. ****, ***, **, * Significantly greater ($P < 0.001$, 0.005, 0.01, 0.05, respectively) than untreated and uncoated (no fibronectin) implants; + significantly greater ($P < 0.05$) than untreated and fibronectin-coated (Fibronectin) implants; [a] significantly greater ($P < 0.05$) than RFGD-treated and uncoated implants at the corresponding time points based on analysis of variance.

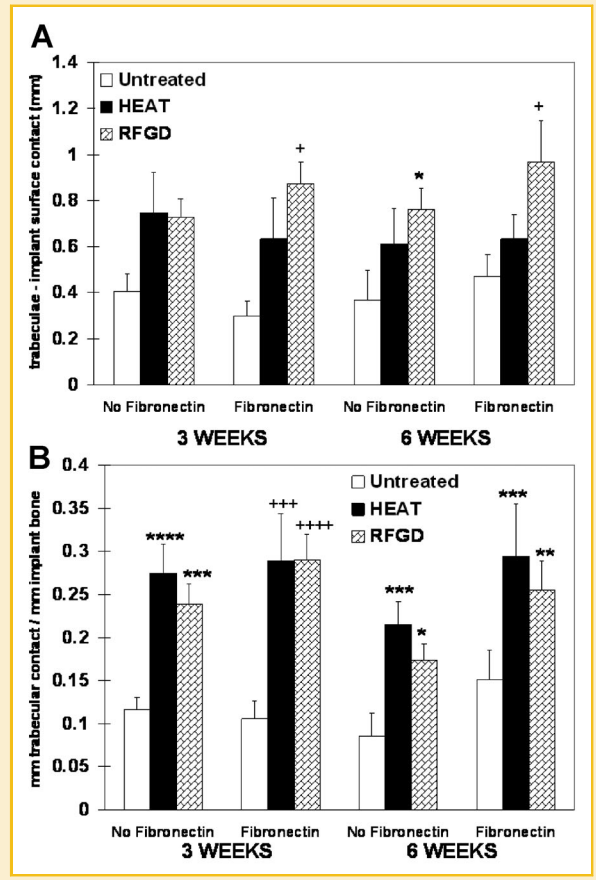

Fig. 3. Effects of heat and RFGD pretreatment of Ti6Al4V on trabeculae–implant surface contact. A: The length (in mm) of trabeculae-to-implant surface contact per cross-section. B: The length (in mm) of trabeculae-to-implant surface contact/length (mm) of implant bone. ****, ***, **, * Significantly greater ($P < 0.001$, 0.005, 0.01, 0.05, respectively) than untreated and uncoated (no fibronectin) implants; ++++, +++, + significantly greater ($P < 0.001$, 0.005, 0.05, respectively) than untreated and fibronectin-coated (fibronectin) implants at the corresponding time points based on analysis of variance.

more pronounced for heat and RFGD-pretreated compared to untreated implants. The quantitative effects of heat pretreatment on implant-trabeculae surface contact/mm of implant bone were equal to or greater than that of RFGD pretreatment (Fig. 3B). No significant differences were found between the 3 and 6 week implants in the trabeculae-to-implant surface contact/mm of implant bone compared under the same experimental conditions.

Implants that underwent heat pretreatment exhibited significantly higher shear strengths compared to RFGD-pretreated or untreated implants (Fig. 4). Average shear strengths for preheated uncoated and fibronectin-coated implants at 3 and 6 weeks were ~3–5-fold higher than those for untreated and RFGD-pretreated alloy specimens. Untreated and RFGD-pretreated implants coated with fibronectin demonstrated modest increases in strength at 6 weeks compared to the corresponding uncoated specimens. The implant-bone shear strengths for each group generally increased from 3 to 6 weeks (Fig. 4).

The number of bonded trabeculae and implant-trabeculae surface contact were also normalized to the area of bone that had formed around the implant's circumference (Fig. 5). The normalized levels were increased significantly ($P < 0.001$–0.05) from two- to threefold by heat or RFGD-pretreatment compared to untreated specimens by 3 weeks (unpublished results) or 6 weeks (Fig. 5). Also, a pattern of higher levels were found for implants coated with fibronectin compared to uncoated implants. Fibronectin's apparent effects on both parameters were greater for RFGD-pretreated implants than for untreated implants (Fig. 5). The effect of heat pretreatment on both parameters in the presence or absence of a fibronectin coating compared to untreated implants were equal to or greater than that of RFGD pretreatment. When the shear strengths for the six groups were plotted against the average normalized number of bonded trabeculae or trabeculae surface contact, linear regression analysis yielded a correlation coefficient of 0.54 (n.s.; insets, Fig. 5).

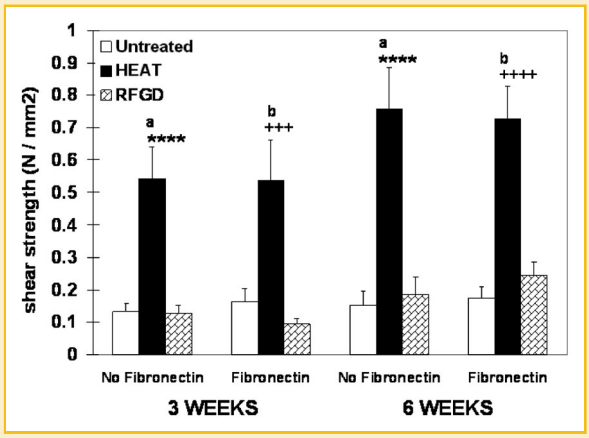

Fig. 4. Effects of heat or RFGD pretreatment of Ti6Al4V implants on implant-femur shear strength for Ti6Al4V implants. **** Significantly greater ($P < 0.001$) than untreated and uncoated (no fibronectin) implants; ++++, +++ significantly greater ($P < 0.001$ and 0.005, respectively) than untreated and fibronectin-coated (Fibronectin) implants; a,b significantly greater ($P < 0.001$) than uncoated and coated RFGD-pretreated implants, respectively, at the corresponding time points based on analysis of variance.

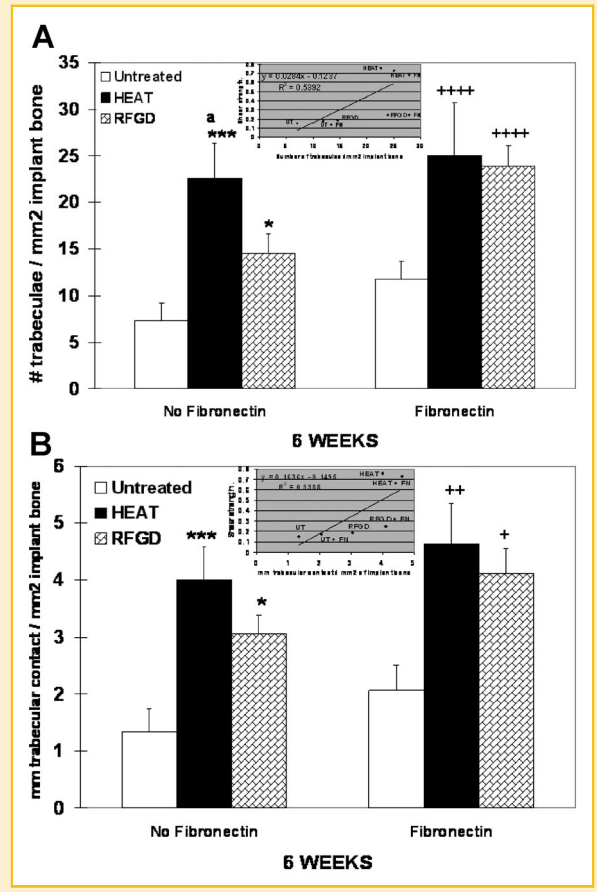

Fig. 5. Effects of heat and RFGD pretreatment of Ti6Al4V on the number of trabeculae bonded to the implant and trabeculae—implant surface contact normalized to the area (in mm^2) of bone circumscribing the implant. A: Number of trabeculae in contact with implant/area (mm^2) of surface implant bone. B: The length of surface contact between trabeculae and implant/area (mm^2) of implant bone. ***, * Significantly greater ($P < 0.005$, 0.05, respectively) than untreated and uncoated (no fibronectin) implants; ++++, ++, + significantly greater ($P < 0.001$, 0.01, 0.05, respectively) than untreated and fibronectin-coated (fibronectin) implants; [a] significantly greater ($P < 0.05$) than RFGD-treated and uncoated implants at the corresponding time points based on analysis of variance. Inset for (A) and (B): average shear strengths for the six experimental groups shown versus number of trabeculae in contact with implant and trabecular surface contact with implant, respectively, each normalized to implant bone area (mm^2). Correlation coefficients (r^2) were calculated by linear regression.

The shear strengths obtained at 6 weeks for the untreated, untreated + fibronectin, RFGD, and RFGD + fibronectin groups were plotted against the corresponding mean values at 6 weeks for the number of bonded trabecular struts and length of trabecular surface contacts before or after these values were normalized to the length and area of implant bone. Linear regression analysis yielded correlation coefficients (r^2) of 0.87–0.99 for all parameters (Fig. 6). In contrast, shear strength was poorly correlated with histomorphometric measures of the bone circumscribing the implants, such as its length ($r^2 = 0.03$) and area ($r^2 = 0.13$).

For fibronectin-coated heat or RFGD-pretreated implant specimens, FTIR analysis revealed that higher levels of acid phosphate were found in trabeculae that bonded to the implant (prior to its removal) compared to the surrounding trabecular or cortical bone (Fig. 7A; white arrows). Fibronectin also appeared to increase the mineral content of acid phosphate and decreased the mineral:matrix ratio in peri-implant trabecular bone adjacent to RFGD-pretreated implants (Fig. 7B; white arrows). Notably, FTIR analysis revealed a general pattern of higher mean acid phosphate content measured in bone close to the implant and in peri-implant bone for fibronectin-coated compared to uncoated implants (Fig. 7).

DISCUSSION

STIMULATION OF OSSEOINTEGRATION BY HEAT AND RFGD PRETREATMENTS IN VIVO

Our major finding is that heat and RFGD pretreatments of a Ti6Al4V implant increased quantitative mechanical and histomorphometric measures of osseointegration in a rat femoral model. The most prominent histomorphometric marker was trabecular remodeling observed in close proximity to the implant that led to the union of trabecular struts with the implant. Two measures of trabecular-implant bonding, the number of trabeculae in contact with the implant and the length of trabeculae-implant surface contact, expressed directly or normalized to the length or area of circumferential implant bone, revealed an invariant pattern in which bonding was markedly enhanced by both pretreatments at 3 or 6 weeks with or without a fibronectin coating. Therefore, our findings establish that the formation of contacts between trabecular struts and the implant bone is stimulated by alterations in the surface oxide promoted by heat and RFGD pretreatments.

Implant-bone shear strength provided a key mechanical marker of osseointegration that, like trabecular remodeling, was also enhanced by our two implant pretreatments. These findings strongly support a causal connection between the development of trabecular contacts

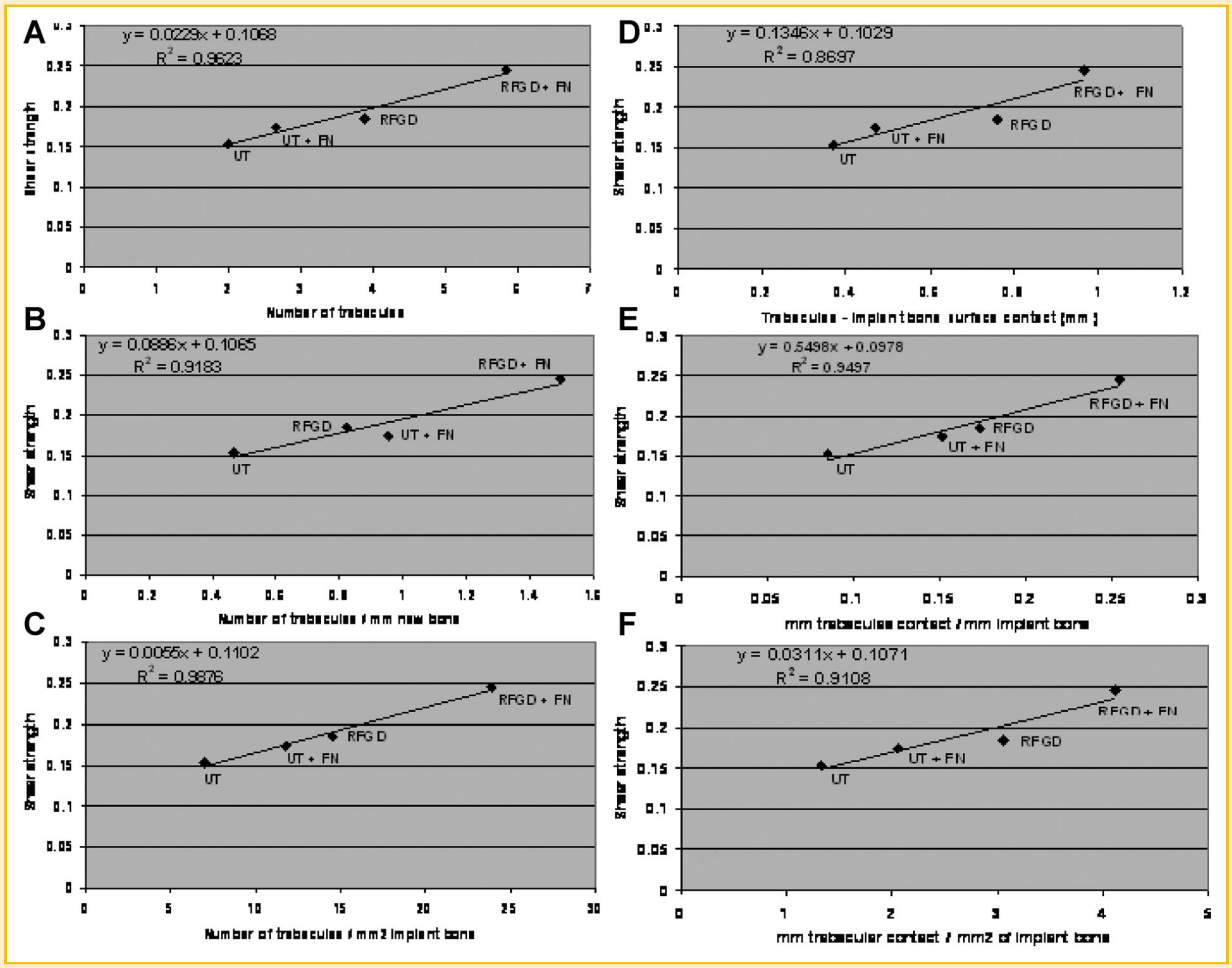

Fig. 6. Linear relationship between implant–femur shear strength and trabecular bonding to implant surface bone. Mean values at 6 weeks for implant–femur shear strength (obtained from Fig. 4) for the untreated (UT), untreated + fibronectin (UT + FN), RFGD (RFGD), and RFGD + fibronectin (RFGD + FN) groups were plotted against the corresponding mean values at 6 weeks for the number of trabeculae bonding to the implant (A) and length (D) of trabecular surface contact with implant; and the number of bonded trabeculae and length of trabecular surface contacts normalized to the circumferential length (B and E, respectively) and area (C and F, respectively) of implant bone (obtained from Figs. 3 and 5). Correlation coefficients (r^2) were calculated by linear regression.

with the untreated and RFGD-pretreated implants and their mechanical bonding to bone within the medullary canal. The linear regression analyses from untreated and RFGD-pretreated specimens also suggest that both fibronectin and the latter pretreatment increase shear strength and trabecular remodeling at the implant surface. It is uncertain whether time points longer than 6 weeks will demonstrate that fibronectin and RFGD pretreatment promote even greater increases in bonding strength compared to earlier times. In comparison, the preheating of Ti6Al4V implants generated three- to fivefold increases in shear strength compared to untreated implants at either 3 or 6 weeks in the presence or absence of a fibronectin coating. Even though the quantitative effects of the two pretreatments on trabecular bonding to implant bone were roughly equivalent, the shear strengths measured for preheated implants were much higher than those exhibited by RFGD-pretreated implants. It is possible that the influence of trabecular contacts on bone-implant bonding strength was augmented by other biomechanical properties of the preheated implant surface. Our results suggest that trabecular bonding plays a role in the effects of both pretreatments on mechanical osseointegration, although the mechanism underlying these effects is likely to be more complex for heat pretreatment.

THE ROLE OF FIBRONECTIN IN THE EFFECTS OF RFGD AND HEAT PRETREATMENTS ON TRABECULAR BONDING AND OSSEOINTEGRATION

In parallel to its stimulatory effects on osteoblast differentiation in vitro [Rapuano et al., 2012b], our current study demonstrated that a fibronectin coating produced a pattern of increases the numbers of trabeculae that bonded to the implant and the levels of implant-trabeculae surface contact in vivo. The effects of fibronectin on trabeculae-implant contacts were generally greater for RFGD-pretreated implants and, in some cases, greater for heat-pretreated implants compared to untreated specimens. When viewed within the context of our in vitro studies [Rapuano et al., 2012b,c], our current results suggest that RFGD pretreatment and, to a lesser extent, heat pretreatment increased trabecular bonding partly by augmenting

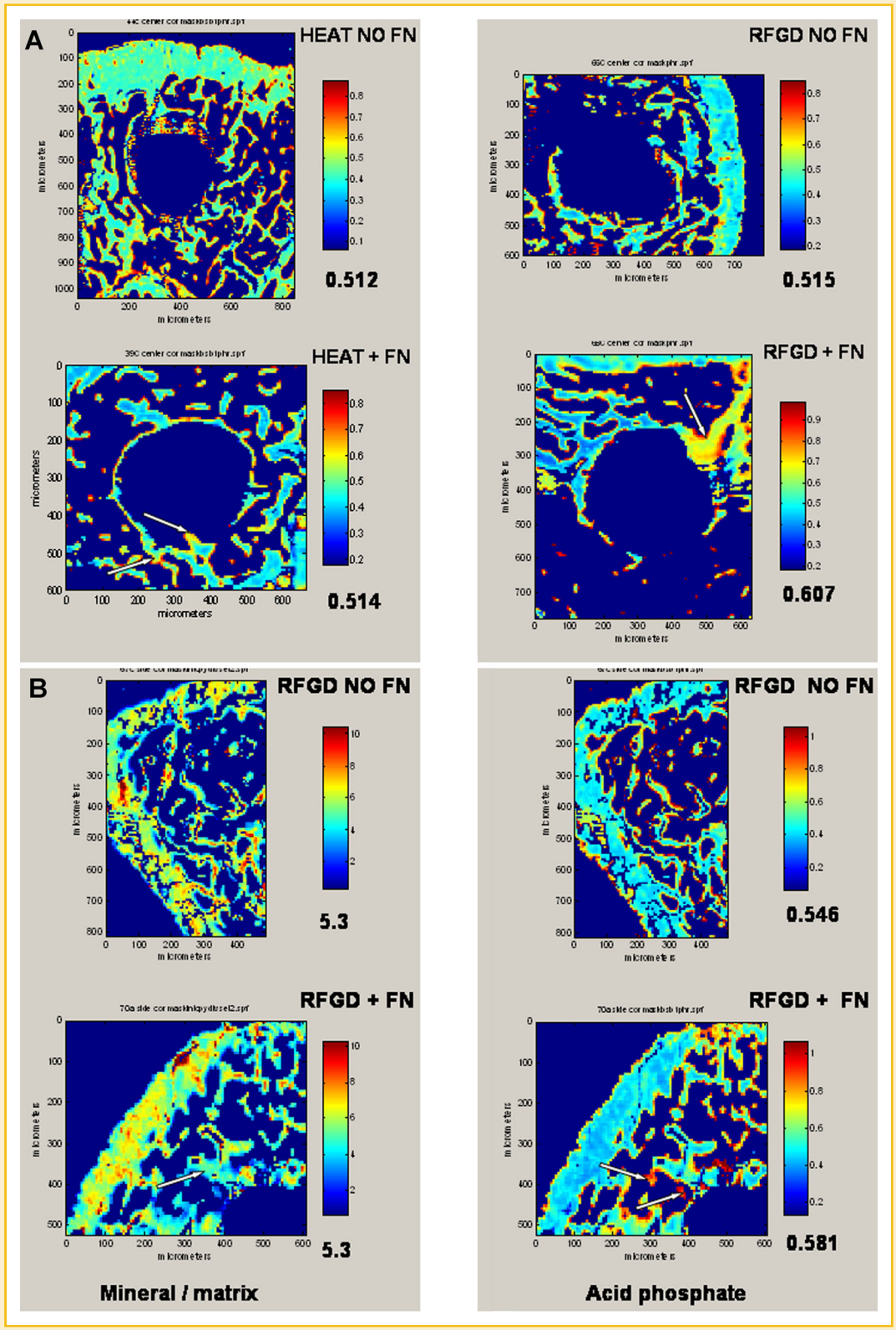

Fig. 7. FTIR spectral color maps of the acid phosphate levels and mineral:matrix ratio in bone adjacent to pretreated implants. A: Acid phosphate levels in bone that was in close proximity to the implant for sections from fibronectin-coated and uncoated heat and RFGD-pretreated implant specimens. B: Acid phosphate levels and mineral:matrix ratio in peri-implant bone for sections from fibronectin-coated and uncoated RFGD-pretreated implant specimens. White arrows denote focal areas of lower mineral:matrix ratio (blue areas) and higher acid phosphate content (red and yellow areas) compared to the surrounding trabecular or cortical bone. Mean values of acid phosphate and mineral:matrix ratio are shown below each spectral map color scale.

adsorbed fibronectin's intrinsic capacity to stimulate the differentiation of osteoblasts on the implant surface. In an osteogenesis-favorable environment, osteblastic cells on the implant surface are thought to be capable of producing a repertoire of paracrine growth factors that would induce differentiation of osteoprogenitor cells in the surrounding tissue to form a mineralized matrix [Kieswetter et al., 1996]. This process would lead to the development of bone from the surrounding distal tissue toward the implant. In a similar manner, an exogenous fibronectin coating may promote remodeling and recruitment to the surface of neighboring trabeculae by stimulating osteoblast differentiation on the surface and the production of osteogenic paracrine factors that act on nearby trabecular cells. This supposition is supported by FTIR findings showing areas of new trabecular bone formation near fibronectin-coated implants signified by higher acid phosphate levels and lower mineral:matrix ratios [Spevak et al., 2013] compared to the surrounding trabecular or cortical bone. Moreover, we have shown that the pretreatments enhance matrix gene/osteoblast marker gene expression [Rapuano et al., 2012c], cell-directed mineralization [Rapuano et al., 2013], and trabecular bonding/implant shear strength (Figs. 2–6) even in the absence of an exogenous fibronectin coating. These latter results suggest that the bioactivities of other endogenous osteogenic proteins that adsorb to the implant surface in vivo are also increased by our pretreatments resulting in downstream effects on osseointegration.

THE COMPARATIVE ROLES OF TRABECULAR BONDING AND IMPLANT SURFACE BONE IN THE EFFECTS OF RFGD AND HEAT PRETREATMENTS ON OSSEOINTEGRATION

Other laboratories reported evidence supporting the role of trabeculae and trabecular remodeling in the osseointegration of implant materials in cancellous bone. Gabet et al. [2006] demonstrated that trabecular bone volume density (BV/TV), trabecular thickness (Tb.Th), trabecular number (Tb.N), and connectivity density were all increased in peri-implant bone by intermittent PTH administration, and that a highly significant correlation existed between biomechanical and morphometric parameters, especially trabecular volume density ($r^2 = 0.72$) and thickness ($r^2 = 0.60$). A multi-variant model of suture anchor pullout strength that was based on trabecular morphometric parameters was also highly correlated ($r^2 = 0.86$) with actual pullout strength [Yakacki et al., 2010]. The results of these studies [Gabet et al., 2006; Yakacki et al., 2010] closely mirror some of the results of the current study. Yet despite the stimulatory effects of our pretreatments on trabecular bonding and its positive correlation with pullout strength, neither pretreatment significantly increased implant surface coverage by bone or its area. In contrast, other studies showed that these latter parameters were increased by implant surface modifications [Weng et al., 2003; Yakacki et al., 2010]. However, the analyses in these studies were made over much longer periods (4–9 months) than those used in the current study. Greater differences between our untreated and pretreated implants in the amount of implant-to-bone contact might be observed at longer time points; it may take as long as 1 year for increases in this measure of integration to appear [Han et al., 1998]. Furthermore, Gabet et al. [2006] found that biomechanical measures of osseointegration were not as well correlated with the volume of bone in contact with the implant compared to trabecular parameters which is similar to the findings of the current study. Therefore, the quantitative and qualitative characteristics of trabeculae that bond to implants inserted into cancellous bone may be more indicative of mechanical osseointegration compared to implant-to-bone surface contact.

EFFECTS OF Ti6AL4V OXIDE PHYSICAL AND CHEMICAL PROPERTIES ON IMPLANT OSSEOINTEGRATION

The differences between the two pretreatments of in their effects on osteoblast marker gene expression [Rapuano et al., 2012c], cell-directed mineralization [Rapuano et al., 2013], and osseointegration may have arisen from the unique physicochemical characteristics of each resultant oxide surface. We found that heat and RFGD pretreatments increased the Ti6Al4V oxide's net surface charge with the latter pretreatment exerting a greater effect [MacDonald et al., 2011]. However, only heat pretreatment also altered oxide elemental composition, roughness, and nanotopography by creating a pattern of oxide elevations ~50–100 nm in diameter [MacDonald et al., 2011] that were also observed on the surface of the Ti6Al4V rods used in our current study. In contrast, the RFGD pretreatment of Ti6Al4V disks did not alter the atomic composition, roughness, or topography of the planar alloy surface [MacDonald et al., 2011] or that of the titanium alloy rods used in the current study.

Previous studies established that "roughened" implant surfaces containing topographical features with mean height and spacing in the micron range exhibit greater interface strength largely due to bone-implant interlocking forces [Cooper, 2000; Chang, 2010]. Surfaces possessing R_a roughness values (arithmetic mean values of the surface departures from the mean plane) $\geq \sim 1–2\ \mu m$ demonstrate bone ingrowth and interlocking [Cooper, 2000; Lang and Jepsen, 2009]. These mechanical and etching microstructures reported by others are 14–40-fold greater in roughness compared to the topographical features created by our heat pretreatment (average roughness = 54–70 nm). Nevertheless, biomechanical properties of the preheated implant's oxide nanotopography may have contributed to its greater shear strength compared to untreated or RFGD-pretreated implants in our study. Diefenbeck et al. [2011] used a plasma chemical oxidation (PCO) treatment of a titanium alloy implant to increase the thickness of the oxide layer to a 4 μM coating containing micropores inside of which calcium and phosphate were deposited. This microporous implant displayed a three- to fourfold increase in shear strength in a rat tibial model compared to a much smoother alloy surface created by PCO followed by blasting with glass microspheres. Our preheated implants also displayed a 3-fold increase in shear strength compared to smoother RFGD-pretreated implants, despite having an oxide layer that lacked the micro level thickness, micropores and embedded electrolytes described by Diefenbeck et al. [2011]. These findings suggest that the increased implant-bone bonding strength promoted by the heat pretreatment-induced oxide nanostructure can be attributed to cooperative or synergistic effects of enhanced formation of trabeculae-implant contacts and mechanical interlocking of the implant with trabecular or other surface bone.

Any potential effects of oxide nanostructure on trabecular osteogenesis likely involves the regulation of osteoblast function. Based on an osteoprogenitor cell size of 5–12 μm in length, it has

been proposed that implant features with dimensions of several microns are optimal for promoting osteoblast differentiation by subjecting the cells to a minor distortional strain [Schwartz et al., 1999]. It is unlikely that the oxide nanostructures present on the preheated Ti6Al4V surface, which are much smaller than 1 μm, can enhance osseointegration by influencing cell differentiation events through distortional signals. However, the preheated surface nanostructures may achieve the same effects by altering the tertiary structure and conformational bioactivities of adsorbed fibronectin and endogenous osteogenic proteins [Webster et al., 2001; Miller et al., 2007] that regulate osteoblastogenesis and the expression of specific osteoblast genes. Conversely. heat and RFGD treatment may exert similar effects on the bioactivities of osteogenic proteins such as fibronectin [Rapuano et al., 2012a] through alterations in surface oxide charge.

Differences between heat and RFGD pretreatment in their effects on osteoblast differentiation that are mediated by distinctive oxide characteristics may be partly responsible for their unequal effects on trabecular bonding and shear strength. We previously found that RFGD pretreatment produced a greater induction of osteopontin and bone sialoprotein genes in osteoprogenitor cells in vitro compared to heat pretreatment [Rapuano et al., 2012c]. In contrast, heat pretreatment increased mRNA levels for alkaline phosphatase and osteocalcin more than RFGD pretreatment [Rapuano et al., 2012c]. Other studies showed that treatments of titanium implants that increase surface roughness, hydrophilicity, or both roughness and hydrophilicity can have different, unpredictable effects on osteoblast gene expression [Zhao et al., 2007; Olivares-Navarrete et al., 2010; Klein et al., 2011], inducing some osteoblast gene markers while repressing others [Zhao et al., 2007]. These findings suggest that changes in surface oxide chemistry and topography interact in a complex manner to coordinately modulate the bioactivities of adsorbed proteins and the expression of specific osteoblast genes, potentially changing biomineralization.

In view of the complex interaction between oxide chemistry and topography in their effects on osteoblast gene expression, the repertoire of paracrine growth factors produced by cells attached to the preheated surface likely differs from that produced by cells attached to RFGD-pretreated implants. This could account for the dissimilarities between the effects of the two pretreatments on measures of osseointegration. For example, fibronectin generally demonstrated a pattern of greater quantitative effects on trabecular parameters for RFGD-pretreated compared to preheated implants. It is possible that fibronectin's effects when coated on preheated implants may have been inhibited by a greater adsorption of other osteogenic proteins that also increase trabecular bonding to the implant. In addition, some of these latter proteins may alter osteoblast growth factor expression to induce changes in the qualitative properties of peri-implant trabecular bone, such as connectivity [Gabet et al., 2006], or the heterogeneity of bone mineral properties [Gourion-Arsiquaud et al., 2013], that lead to increases in mechanical shear strength. Future studies will examine the comparative effects of heat and RFGD pretreatments of Ti6Al4V on the qualitative bone mineral properties of trabeculae bonding to the implant and the bone circumscribing it in relationship to the differential effects of the pretreatments on mechanical osseointegration.

ACKNOWLEDGMENTS

The sponsor did not have any role in the study design; the collection, analysis and interpretation of data; the writing of the report; or the decision to submit the article for publication. This material also resulted from work supported with resources and the use of facilities at the James J. Peters VA Medical Center, Bronx, New York. This investigation was also conducted at the HSS research facility constructed with support of Grant C06-RR12538-01 from the National Center for Research Resources, NIH. We thank Dr. Hannes Schniepp for the AFM surface analyses, Dr. Stephen Doty, and Tony Labissiere for technical assistance with the SEM analyses, Dr. Adele Boskey and Lyudmila Spevak for assistance with FTIR, and Kyle Hackshaw, Carrie Guan, and Jenny Lee for help with preparation of the alloy implants.

REFERENCES

Adell R, Eriksen B, Lekholm U, Brånemark PI, Jemt T. 1990. A long-term follow-up study of osseointegrated implants in the treatment of totally edentulous jaws. Int J Oral Maxillofac Implants 5:347–359.

Barber TA, Ho JE, DeRanieri A, Virdi AS, Sumner DR, Healy KE. 2007. Peri-implant bone formation and implant integration strength of peptide-modified p(AAM-co-EG/AAC) interpenetrating polymer network-coated titanium implants. J Biomed Mater Res A 80:306–320.

Boskey A, Mendelsohn R. 2005. Infrared analysis of bone in health and disease. J Biomed Opt 10:31–102.

Chang P-C. 2010. Evaluation of functional dynamics during osseointegration and regeneration associated with oral implants: A review. Clin Oral Implants Res 21(1):1–12.

Cooper LF. 2000. A role for surface topography in creating and maintaining bone at titanium endosseous implants. J Prosth Dent 84:522–534.

Dhert WJ, Thomsen P, Blomgren AK, Esposito M, Ericson LE, Verbout AJ. 1998. Integration of press-fit implants in cortical bone: A study on interface kinetics. J Biomed Mater Res 41:574–583.

Diefenbeck M, Mückley T, Schrader C, Schmidt J, Zankovych S, Bossert J, Jandt KD, Faucon M, Finger U. 2011. The effect of plasma chemical oxidation of titanium alloy on bone-implant contact in rats. Biomaterials 32:8041–8047.

Dohan Ehrenfest DM, Coelho PG, Kang BS, Sul BYT, Albrektsson T. 2010. Classification of osseointegrated implant surfaces: Materials, chemistry and topography. Trends Biotechnol 28(4):198–206.

Erben RG. 1997. Embedding of bone samples in methylmethacrylate: An improved method suitable for bone histomorphometry, histochemistry, and immunohistochemistry. J Histochem Cytochem 45(2):307–313.

Gabet Y, Muller R, Levy J, Dimarchi R, Corev M, Bab I, Kohavi D. 2006. Parathyroid hormone 1-34 enhances titanium implant anchorage in low-density trabecular bone: A correlative micro-computed tomographic and biomechanical analysis. Bone 39:276–282.

Gourion-Arsiquaud S, Lukashova L, Power J, Loveridge N, Reeve J, Boskey AL. 2013. Fourier transform infrared imaging of femoral neck bone: Reduced heterogeneity of mineral-to-matrix and carbonate-to-phosphate and more variable crystallinity in treatment-naive fracture cases compared with fracture-free controls. J Bone Miner Res 28(1):150–161.

Grossmann Y, Levin L. 2007. Success and survival of single dental implants placed in sites of previously failed implants. J Periodontol 78:1670–1674.

Han CH, Johansson CB, Wennerberg A, Albrekisson T. 1998. Quantitative and qualitative investigation of surface enlarged titanium and titanium alloy implants. Clin Oral Implants Res 9:1–10.

Harbers GM, Healy KE. 2005. The effect of ligand type and density on osteoblast adhesion, proliferation, and matrix mineralization. J Biomed Mater Res 75:855–869.

Hardt CR, Grondahl K, Lekholm U, Wennstrom JL. 2002. Outcome of implant therapy inrelation to experienced loss of periodontal bone support: A retrospective 5-year study. Clin Oral Implants Res 13:488–494.

Imam MA, Fraker AC. 1996. Titanium alloys as implant materials. In: Brown SA, Lemons JE, editors. Medical applications of titanium and its alloys. Philadelphia: American Society for Testing and Materials. pp 3–16.

Johansson P, Strid KG. 1994. Assessment of bone quality from cutting resistance during implant surgery. Int J Oral Maxillofac Implants 9: 279–288.

Kasemo B. 1983. Biocompatibility of titanium implants: Surface science aspects. J Prosthetic Dent 49:832–837.

Kieswetter K, Schwartz Z, Dean DD, Boyan BD. 1996. The role of implant surface characteristics in the healing of bone. Crit Rev Oral Biol Med 7(4): 329–345.

Klein MO, Bijelic A, Ziebart T, Koch F, KÃmmerer PW, Wieland M, Konerding MA, Al-Nawas B. 2011. Submicron scale-structured hydrophilic titanium surfaces promote early osteogenic gene response for cell adhesion and cell differentiation. Clin Implant Dent Relat Res. DOI: 10.1111/j.1708-8208.00339.x.[Epub ahead of print]

Lang NP, Jepsen S. 2009. Implant surfaces and design. Consensus report of working group 4. Clin Oral Implants Res 20:230–233.

Larsson G, Thomsen P, Aronsson BO, Rodahl M, Lausmaa J, Kasemo B, Ericson LE. 1996. Bone response to surface-modified titanium implants: Studies on the early tissue response to machined and electropolished implants with different oxide thicknesses. Biomaterials 17:605-616.

Lausmaa J. 2001. Mechanical, thermal, chemical and electrochemical surface treatment of titanium. In: Brunette DM, Tengvall P, Textor M, Thomsen P, editors. Titanium in medicine: Material science, surface science, engineering, biological responses and medical applications. New York: Springer. pp 232–266.

MacDonald DE, Markovic B, Allen M, Somasundaran P, Boskey AL. 1998. Surface analysis of human plasma fibronectin adsorbed to commercially pure titanium materials. J Biomed Mater Res 41:120–130.

MacDonald DE, Betts F, Doty SB, Boskey AL. 2000. A methodological study for the analysis of apatite-coated dental implants retrieved from humans. Ann Periodontol 5:175–184.

MacDonald DE, Betts F, Stranick M, Doty S, Boskey AL. 2001. Physiochemical study of plasma-sprayed hydroxyapatite-coated implants in humans. J Biomed Mater Res 54:480–490.

MacDonald DE, Deo N, Markovic B, Stranick M, Somasundaran P. 2002. Adsorption and dissolution behavior of human plasma fibronectin on thermally and chemically modified titanium dioxide particles. Biomaterials 23:1269–1279.

MacDonald DE, Rapuano BE, Deo N, Stranick M, Somasundaran P, Boskey AL. 2004. Thermal and chemical modification of titanium–aluminum–vanadium implant materials: Effects on surface properties, glycoprotein adsorption, and MG63 cell attachment. Biomaterials 25:3135–3146.

MacDonald DE, Rapuano BE, Schniepp HC. 2011. Surface oxide net charge of a titanium alloy: Comparison between effects of treatment with heat or radiofrequency plasma glow discharge. Colloids and Surface B Biointerfaces 82:173–181.

Machtei EE, Mahler D, Oettinger-Barak O, Zuabi O, Horwitz J. 2008. Dental implants placed in previously failed sites: Survival rate and factors affecting the outcome. Clin Oral Implants Res 19:259–264.

Machtei EE, Horwitz J, Mahler D, Grossmann Y, Levin L. 2011. Third attempt to place implants in sites where previous surgeries have failed. J Clin Periodontol 38(2):195–198.

Mendonca G, Mendonca DBS, Aragao FJL, Cooper LF. 2008. Advancing dental implant surface technology—From micron-to nanotopography. Biomaterials 29:3822–3835.

Miller DC, Haberstroh KM, Webster TJ. 2007. PLGA nanometer surface features manipulate fibronectin interactions for improved vascular cell adhesion. J Biomed Mater Res 81A:678–684.

Morris HF, Winkler S, Ochi S. 2001. A 48-month multicenter clinical investigation: Implant design and survival. J Oral Implantol 27:180–186.

Moursi AM, Damsky CH, Lull J, Zimmerman D, Doty SB, Aota S, Globus RK. 1996. Fibronectin regulates calvarial osteoblast differentiation. J Cell Sci 109:1369–1390.

Olivares-Navarrete R, Hyzy SL, Hutton DL, Erdman CP, Wieland M, Boyan BD, Schwartz Z. 2010. Direct and indirect effects of microstructured titanium substrates on the induction of mesenchymal stem cell differentiation towards the osteoblast lineage. Biomaterials 31(10):2728–2735.

Rapuano BE, MacDonald DE. 2011. Surface oxide net charge of a titanium alloy. Modulation of fibronectin-activated attachment and spreading of osteogenic cells. Colloids and Surface B Biointerfaces 82:95–103.

Rapuano BE, Wu C, MacDonald DE. 2004. Osteoblast-like cell adhesion to bone sialoprotein peptides. J Orthop Res 22:353–361.

Rapuano BE, Lee JJ, MacDonald DE. 2012a. Titanium alloy surface oxide modulates the conformation of adsorbed fibronectin to enhance its binding to $\alpha5\beta1$ integrins in osteoblasts. Eur J Oral Sci 120(3):185–194.

Rapuano BE, Hackshaw KM, MacDonald DE. 2012b. Surface coating of a titanium alloy with fibronectin augments expression of osteoblast gene markers in the MC3T3 osteoprogenitor cell line. J Oral Maxillofacial Implants 27(5):1081–1090.

Rapuano BE, Hackshaw K, Macdonald DE. 2012c. Heat or radiofrequency glow discharge pretreatment of a titanium alloy stimulates osteoblast gene expression in the MC3T3 osteoprogenitor cell line. J Periodontal Implant Sci 42(3):95–104.

Rapuano BE, Singh H, Boskey AL, Doty SB, MacDonald DE. 2013. Effects of heat and radiofrequency plasma glow discharge pretreatment of a titanium alloy on mineral formation in MC3T3 osteoprogenitor cell cultures: Evidence for enhanced osteoinductive properties. J Cell Biochem doi: 10.1002/jcb.24536 [Epub ahead of print] PMID: 23494951.

Schwartz Z, Lohmann CH, Oefinger J, Bonewald LF, Dean DD, Boyan BD. 1999. Implant surface characteristics modulate differentiation behavior of cells in the osteoblastic lineage. Adv Dent Res 13:38–48.

Sousa SR, Lamghari M, Sampaio P, Moradas-Ferreira P, Barbosa MA. 2008. Osteoblast adhesion and morphology on TiO2 depends on the competitive preadsorption of albumin and fibronectin. J Biomed Mater Res A 84:281–290.

Spevak L, Flach CR, Hunter T, Mendelsohn R, Boskey A. 2013. Fourier transform infrared spectroscopic imaging parameters describing acid phosphate substitution in biologic hydroxyapatite. Calcif Tissue Int 92(5):418–428.

Webster TJ. 2003. Nanophase ceramics as improved bone tissue engineering materials. Am Ceram Soc Bull 82:1–8.

Webster TJ, Schadler LS, Siegel RW, Bizios R. 2001. Mechanisms of enhanced osteoblast adhesion on nanophase alumina involve vitronectin. Tissue Eng 7(3):291–301.

Weng D, Hoffmeyer M, Hurzeler MB, Richter EJ. 2003. Osseotite vs. machined surface in poor bone quality A study in dogs. Clin Oral Implants Res 14: 703–708.

Yakacki CM, Poukalova M, Guldberg RE, Lin A, Saing M, Gillogly S, Gall K. 2010. The effect of the trabecular microstructure on the pullout strength of suture anchors. J Biomechanics 43:1953–1959.

Zhao G, Raines AL, Wieland M, Schwartz Z, Boyan BDBD. 2007. Requirement for both micron and submicron scale structure for synergistic responses of osteoblasts to substrate surface energy and topography. Biomaterials 28(18): 2821–2829.